Proteome-Driven Elucidation of Adaptive Responses to Combined Vitamin E and C Deficiency in Zebrafish

Ievgen Motorykin,[†] Maret G. Traber,[‡] Robert L. Tanguay,[§] and Claudia S. Maier*,[†]

[†]Department of Chemistry, Oregon State University, 153 Gilbert Hall, Corvallis, Oregon 97331, United States

[‡]Linus Pauling Institute and School of Biological and Population Health Sciences, Oregon State University, 307 Linus Pauling Science Center, Corvallis, Oregon 97331, United States

[§]Department of Environmental and Molecular Toxicology, Oregon State University, 1007 Agriculture & Life Sciences Building, Corvallis, Oregon 97331, United States

Ⓢ *Supporting Information*

ABSTRACT: The purpose of this study was to determine the system-wide consequences of deficiencies in two essential micronutrients, vitamins E and C, on the proteome using zebrafish (*Danio rerio*) as one of the few vertebrate models that similar to humans cannot synthesize vitamin C. We describe a label-free proteomics workflow to detect changes in protein abundance estimates dependent on vitamin regimes. We used ion-mobility-enhanced data-independent tandem mass spectrometry to determine differential regulation of proteins in response to low dietary levels of vitamin C with or without vitamin E. The detection limit of the method was as low as 20 amol, and the dynamic range was five orders of magnitude for the protein-level estimates. On the basis of the quantitative changes obtained, we built a network of protein interactions that reflect the whole organism's response to vitamin C deficiency. The proteomics-driven study revealed that in vitamin-E-deficient fish, vitamin C deficiency is associated with induction of stress response, astrogliosis, and a shift from glycolysis to glutaminolysis as an alternative mechanism to satisfy cellular energy requirements.

KEYWORDS: *vitamin C, vitamin E, ion mobility, MS[E], label-free quantification, zebrafish, glycolysis, glutaminolysis*
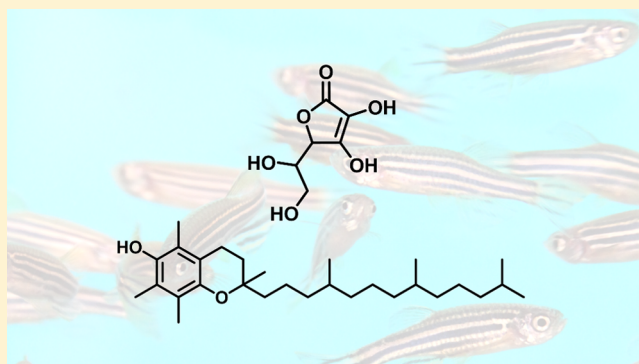
■ INTRODUCTION

The purpose of this study was to determine the consequences of deficiencies in dietary antioxidants, vitamins C and E, on the zebrafish proteome composition. The combination of deficiencies was used because this dietary manipulation is known to cause severe abnormalities.[1,2] Protein abundance estimates were obtained by label-free accurate quantification based on data-independent (MS[E]) acquisition. Functional interpretation of the systems-wide proteome responses revealed the biomolecular networks affected by vitamin C and E deficiency.

In zebrafish, the lack of vitamin E potentiates vitamin C deficiency and causes degenerative myopathy.[3] The classical roles of vitamin C (ascorbic acid, AA) are in maintaining redox homeostasis[4−6] and facilitating the recycling of vitamin E.[7,8] More recently, vitamin C has been identified as an essential cofactor for multiple enzymes involved in the hydroxylation of procollagen[9,10] and several dioxygenases that are involved in maintaining endothelial function with relevance to atherosclerosis[11] and sepsis.[12,13] Inadequate vitamin C levels, potentially leading to hypovitaminosis, remain widespread health concerns in humans affecting particularly under-privileged populations. Recent research indicates that smok-

ing[14] and Western diets rich in fat and cholesterol[15] exacerbate vitamin C deficiency.

In most animals, vitamin C is synthesized in the liver or kidneys and transferred to tissues via circulation.[16,17] Humans are not capable of synthesizing ascorbic acid due to the lack of the functional gene for L-gulonolactone oxidase.[18,19] For studying the effect of vitamin C deficiency, the most widely used animal model is the guinea pig that similarly to humans cannot synthesize vitamin C.[20] The gulonolactone oxidase knockout (Gulo^{−/−}) mouse is an established transgenic animal model for deciphering the physiological roles of vitamin C.[21,22] Similarly to humans, zebrafish also cannot synthesize vitamin C.[23−28] A first report using MS-based metabolomics to study the effect of vitamin C deficiency in zebrafish revealed that vitamin C deficiency affects the purine metabolism.[29] A classical antioxidant function of vitamin C entails the recycling of the tocopheroxyl radical that is generated when vitamin E (α-tocopherol, α-T) functions as a peroxyl radical, chain-breaking antioxidant.[30,31] To evaluate the interrelating roles of vitamins

C and E, we used a 2 × 2 design in the present study resulting in four dietary groups, namely, vitamin-E- and -C-adequate (E+C+), vitamin-E- and -C-inadequate (E−C−), vitamin-C-adequate but inadequate in vitamin E (E−C+), and vitamin-C-inadequate but adequate in vitamin E (E+C−). We subsequently applied a label-free comparative proteomics approach for examining the systems-wide consequences of the different vitamin regimes in adult zebrafish.

In a typical "bottom-up" shotgun experiment, a protein mixture is proteolytically digested with a protease, such as trypsin, to create peptides for further analysis. Liquid chromatography in combination with tandem mass spectrometry (LC−MS/MS) has become the predominantly used technique to both qualitatively and quantitatively analyze a complex mixture of peptides.[32−34] The peptides are chromatographically separated using reversed-phase (RP) chromatography and subsequently subjected to collision-induced dissociation (CID) in a tandem mass spectrometer. The product ion spectra are searched against protein sequence databases to identify the peptides. Unlike comparative isotope-coded labeling methods (e.g., ICAT or iTRAQ), label-free mass spectrometry-based quantitative proteomic approaches are based on the fact that in electrospray ionization (ESI) the peak signal intensity is linearly proportional to the concentration of a peptide (over an approximate range of 5−5000 fmol).[35,36] Currently, two acquisition techniques have been technically realized and applied for detecting and quantifying peptides, namely, data-dependent acquisitions (DDAs) and data-independent acquisitions (DIAs).

Data-dependent acquisitions are based on tracking of precursor ion intensities on-the-go.[37] The peptide precursor ions that fulfill preselected features are sequentially subjected to MS/MS during the time course of the chromatography. Proteolytic digests in proteomics-type workflow are often complex and even when using ultraperformance liquid chromatography (UPLC) at every moment multiple peptides coelute. In DDA techniques, survey scan and MS/MS scans are used sequentially and compete for duty cycle time. Therefore, both the number of the most intense peaks subjected to MS/MS analysis and the timespan of a survey scan need to be optimized to acquire accurate mass information for the peptide precursor ions and to ensure information-rich fragment ion spectra.[38,39] Albeit somewhat dependent on the mass-spectrometry platform used, a possible caveat of DDAs is that a substantial portion of the acquisition cycle is spent acquiring fragment ion spectra; therefore, the intensities of the peptide ions are measured inaccurately and, consequently, are less suited for estimating peptide abundances.[39]

DIA techniques perform parallel fragmentation of precursor ions, meaning that all peptide precursors are fragmented simultaneously regardless of their characteristics. For proteomic-type applications, currently most DIAs are realized by coupling nanoUPLC systems to high-resolution quadrupole time-of-flight (Q-TOF) mass spectrometers. This combination of equipment takes advantage of the high peak and separation capacity of UPLCs and the measurement of precursor and product ions with accurate mass. In the DIA mode, the Q-TOF mass spectrometer conducts a low-energy MS scan providing access to precursor ion mass and intensity data for quantitation and an elevated energy scan to obtain product ion information. A critical post acquisition step of the DIA technique is the alignment of the fragment ions with the respective precursor ion. DIA-based acquisitions enable quantification based on the peptide ion intensities. The estimation of protein abundance is based on the observation that the average signal intensity of the three most intense tryptic peptides relates to the protein abundance level regardless of protein size.[40] The estimation of protein levels (moles of each identified protein) is based on using an internal protein standard (spiked in at a defined amount).

Recently, a commercially available hybrid high-resolution ion mobility quadrupole time-of-flight (IM-Q-TOF) mass spectrometry system that enables the acquisition of ion mobility-enhanced DIA (aka IM-MS^E) data has become available.[41] In this instrument configuration, ions are separated according to their velocity with which they transverse the traveling wave ion mobility device. Parameters that affect the ion's mobility are its charge, size, and shape.[42] In ion mobility-enhanced MS^E acquisitions, ions are separated according to their mobility and then dependent on the energy regime applied in the transfer region directly passed on to the TOF analyzer or collisionally dissociated, and the resulting fragment ions are measured in the TOF analyzer. In the IM-MS^E mode, fragment ions are drift time-aligned with their precursors. An often touted advantage of ion mobility-enhanced MS^E acquisitions is the orthogonal separation space gained additionally to the chromatographic separation of the peptides prior to collision-induced dissociation leading to spectral decongestion, improved peptide detection, and dynamic range, all leading cooperatively to more protein identifications.[43]

To investigate the consequences of the combination of vitamin E and C deficiency on protein networks in zebrafish, we profiled the changes in protein abundances. The observed proteome changes were then statistically evaluated and functionally annotated. The protein expression data were used for constructing a protein interaction network. Subnetworks were extracted that comprised proteins related to stress response, glycolysis, and TCA cycles. The observed changes in protein abundances for zebrafish deficient in vitamins E and C suggest a metabolic switch from glycolysis to glutaminolysis as a means of alternative energy production.

■ MATERIALS AND METHODS

Chemicals

Dithiolthreitol (DTT) and iodoacetamide were purchased from Bio-Rad (Hercules, CA). MS-grade water, acetonitrile, and formic acid (99%) were obtained from EMD Chemicals (Gibbstown, NJ). Sequencing-grade trypsin, resuspension buffer, and protease MAX solution were purchased from Promega (Madison, WI). [Glu^1]-fibrinopeptide B ([Glu^1]-Fib) and *Saccharomyces cerevisiae* enolase digest were obtained from Waters (Milford, MA). PBS solution was purchased from Fisher (Fair Lawn, NJ).

Fish Husbandry

Housing of the wild-type tropical 5D strain zebrafish was carried out in the Sinnhuber Aquatic Research Laboratory at Oregon State University, Corvallis, Oregon. The study was performed according to protocols approved by the Institutional Animal Care and Use Committee (IACUC).[44]

Feeding Experiment

The experiment was designed to allow analyzing changes to the proteome upon vitamin C supplementation of fish that were vitamin-E-adequate or -deficient. To do that, we fed fish with predefined diets as previously described.[29] In brief, at 42 days of

age, 40 fish were divided in two groups and fed diets low in vitamin C (C−, 50 mg AA/kg diet, added as Stay-C, DSM Nutritional Products, Parsippany, NJ) with vitamin E at sufficient levels (E+, 178 μmol RRR-α-tocopherol/kg diet) or deficient levels (E−, 22 μmol RRR-α-tocopherol/kg diet). Thus, two vitamin groups were created: E+C− and E−C− with 20 fish in each group. Induction of vitamin C deficiency continued for 56 days, after which half of the fish population in each group was harvested. The diet of remaining fish was altered to have a high amount of vitamin C (C+, 350 mg AA/kg diet, added as Stay-C), thus creating another two vitamin groups: E+C+ and E−C+. After an additional 21 days, the fish were harvested. Thus, four groups with 10 fish in each were created, each having different vitamins levels that varied with supplementation: E+C+, E−C+, E+C−, and E−C− (Supporting Information, Figure S1). Vitamin E and C concentrations have been published.[29]

Protein Extraction and Digestion

Each sample consisted of one whole flash-frozen fish. The whole flash-frozen fish was individually ground under liquid nitrogen using a mortar and pestle. The pipetting scheme used for preparing the protein extracts and digests for each sample is provided in the Supporting Information, Table S1. While still dry, the fish powder was transferred to a microcentrifuge tube and weighed (Supporting Information, Table S1, column 2). A PBS solution with ProteaseMAX (0.04%) was added to the microtubes for the extraction of proteins; assuming the density as 1 mg/mL, its volume was adjusted to six times the fish weight (Supporting Information, Table S1, column 5). The tubes containing the fish powder suspensions were submitted to three freeze−thaw cycles that included flash-freezing in liquid nitrogen for 2 min, thawing for 5 min, and sonicating for 15 min. After lysis, tubes were centrifuged at 4 °C for 10 min at 15 000 relative centrifugal force (rcf), and the supernatants were transferred to new microcentrifuge tubes (1.3 mL) while solid residue was discarded. The sample preparation workflow is shown in Supporting Information, Figure S2.

The concentration of proteins in each sample was determined by a photometric (Bradford) assay (Supporting Information, Table S1, column 6). Proteins in each sample were digested according to the manufacturer's protocol (Promega). The pipetting scheme for preparing the digest of each sample is outlined in Supporting Information, Table S1, columns 7−9. In brief, a volume of solution containing 50 μg of proteins was taken to 93.5 μL with a freshly prepared 50 mM NH$_4$HCO$_3$. Next, 1 μL of 0.5 M DTT (in Millipore water) was added to each vial, and solutions were incubated at 56 °C for 20 min. Then, 2.7 μL of 0.55 M iodoacetamide (in 50 mM NH$_4$HCO$_3$) was added, and solutions were incubated at room temperature in the dark for 15 min. For protein digestion, 1 μL of 1% ProteaseMAX Surfactant in (in 50 mM NH$_4$HCO$_3$) and 1.8 μL of trypsin (1 μg/μL in 50 mM acetic acid) were added. Solutions were incubated at 37 °C for 3 h. The final volume of each solution of digested proteins was 100 μL. Solutions were centrifuged at 12 000 rcf for 10 s, and trifluoroacetic acid (TFA) was added at a final concentration of 0.5%. After snap-freezing in liquid nitrogen, samples were stored at −20 °C until analyzed. At the end, we conducted LC−IM−MS^E analyses of 8, 10, 10, and 9 samples of groups E+C+, E−C+, E+C−, and E−C−, respectively (Supporting Information, Table S1).

Liquid Chromatography−Mass Spectrometry

The analysis of all samples was performed using a Synapt G2 hybrid quadrupole time-of-flight mass spectrometer (Waters, Milford, MA) controlled by MassLynx 4.2 software (Waters). The sample peptide solution (9 μL) was mixed with 1 μL of internal standard (*Saccharomyces cerevisiae* enolase digest, 1 pmol/μL). With 1 μL injection volume the amount of the internal standard per injection on column was 100 fmol. Peptides were separated with a nanoAcquity Ultra Performance LC system (Waters, Milford, MA) equipped with 100 μm × 100 mm BEH130 C18 column with a particle size of 1.7 μm (Waters, Milford, MA). The mobile phase A consisted of 0.1% formic acid in water, and B consisted of 0.1% formic acid in acetonitrile. Each sample was first retained on a trapping column and then washed using 99.5% A for 3 min at a flow rate 5 μL/min. Peptides were separated using a 120 min gradient (3−40% B for 90 min, 40−90% for 2 min, 90% B for 1 min, 90−3% B for 2 min, and 3% B for 25 min) and then electrosprayed into the mass spectrometer, fitted with a nanoSpray source, at a flow rate of 400 nL/min. External calibration of the TOF analyzer was performed using NaI solution over the range of m/z 50 to 2000. The instrument operated in positive V-mode over the calibration range. Mass spectra were acquired in the MS^E mode alternating between a low energy scan (6 eV) to acquire peptide precursor data and a high-energy scan (ramping from 27 to 50 eV) to acquire fragmentation data. The capillary voltage was 2.5 kV, and the source temperature was 40 °C. Scan time was 1.25 s. The instrument settings are listed in Table S2 (Supporting Information). An auxiliary pump delivered a [Glu^1]-Fib solution as an external calibrant (lock-mass) with a concentration of 500 fmol/μL at a rate of 0.2 μL/min. For lock mass acquisition, a low-energy scan was acquired for 0.75 s every 60 s throughout a run.

Peak Detection

Elevated energy mass spectra were extracted, charge-state-deconvoluted, deisotoped, and lock-mass-corrected with [Glu^1]-Fib (MH$^+$ m/z 785.8426). All ion mobility-MS^E samples were analyzed using Identity^E by ProteinLynx Global Server (PLGS) version 2.5 (Waters Corporation, Milford, MA). The following processing parameters and their respective settings were used: chromatographic peak width and MS TOF resolution, automatic; low-energy threshold, 100 counts; elevated energy threshold, 10 counts; intensity threshold, 750 counts.

Protein Database Search

Waters' Identity^E was configured to search *Danio rerio* protein database (26 812 entries) with the digestion enzyme trypsin. The database was modified by adding the yeast enolase sequence (ENO1_YEAST, accession number P00924, Uniprot) that was spiked in as internal standard to facilitate label-free quantification. Identity^E searched the protein database with a fragment ion mass tolerance of 0.025 Da and a parent ion tolerance of 0.0100 Da. The iodoacetamide derivative of cysteine and the oxidation of methionine were specified as variable modifications of amino acids in Identity^E.

Protein Identification, Quantification, and Validation

Scaffold (version 3.3.1, Proteome Software, Portland, OR) was used to validate MS^E-based peptide and protein identifications. Peptide probabilities were assigned by the Peptide Prophet algorithm.[45] Protein probabilities were assigned by the Protein

Prophet algorithm.[46] Proteins that contained similar peptides and could not be differentiated based on MS/MS analysis alone were grouped to satisfy the principles of parsimony. The peptide and protein probabilities were adjusted to allow the best quantification of proteins and keeping the false identification rates at low levels. For each sample, the numbers of peptides assigned with high confidence are compiled in Table S3 (Supporting Information). In addition, Supporting Information Table S5 compiles proteins identified, unique peptides assigned per protein, and protein sequence coverage. This information was directly obtained from Scaffold.

The average of intensity of the three most intense peptides of each protein was normalized to that of the internal standard with an assigned amount of 100 fmol. Proteins could not be quantified if they ambiguously shared peptides that cannot be uniquely attributed to one protein. Ultimately, the information about group name, sample name, protein ID, and quantitative values for proteins was acquired from Scaffold and exported to spreadsheets. The data were then imported into Perseus (http://www.perseus-framework.org/) and statistically analyzed. Perseus was developed by the Max Planck Institute of Biochemistry, Martinsried, Germany and designed to perform all downstream bioinformatics and statistics on proteomics output tables.

Western Blot

Three samples were randomly selected from each group. Samples were prepared for Western Blot analyses by diluting with sample buffer (5% mercaptoethanol in Laemmli buffer, Bio-Rad, Hercules, CA) to a concentration of 1 mg/mL of protein. For SDS-PAGE analysis, 20 μg (20 μL) of proteins was loaded into a precasted 10% gel (Bio-Rad). After electrotransfer to a nitrocellulose (NC) membrane (Bio-Rad), the latter was blocked overnight in 5% nonfat milk in TBS-T (10 mM Tris, pH 8, 150 mM NaCl, 0.05% Tween). The NC paper was blotted for 1 h with antibodies (Thermo, Rockford, IL) against pyruvate kinase M2 (Pkm2), glutamate dehydrogenase (Glud1), and glial fibrillary acidic protein (Gfap). A horseradish-peroxidase-labeled antigoat and antirabbit IgG (Bio-Rad) and an enhanced chemoluminescence kit (SuperSignal West Pico Chemiluminescent Substrate, Thermo) were used to detect signals on a film (Kodak, Rochester, NY). The molecular mass of a protein was estimated using a protein molecular standard (Bio-Rad).

Network Construction

To construct the vitamin-C-deficiency network, protein IDs were uploaded to STRING, Search Tool for the Retrieval of Interacting Genes (www.string-db.org).[47] The data found on protein interactions and the scores information were extracted. The protein network was constructed based on protein interactions using Cytoscape 2.8.2 (The Cytoscape Consortium). The latter is an open-source platform for complex network analysis and visualization.[48]

■ RESULTS AND DISCUSSION

Overall Design and Strategy Applied for the Label-Free Quantitative Proteomic Study

The goal of this study was to investigate the consequences of vitamin E and C deficiency on the zebrafish proteome. The analysis and validation of quantitative bottom-up shotgun proteomics data sets depend critically on the optimal combination of data processing software tools because each
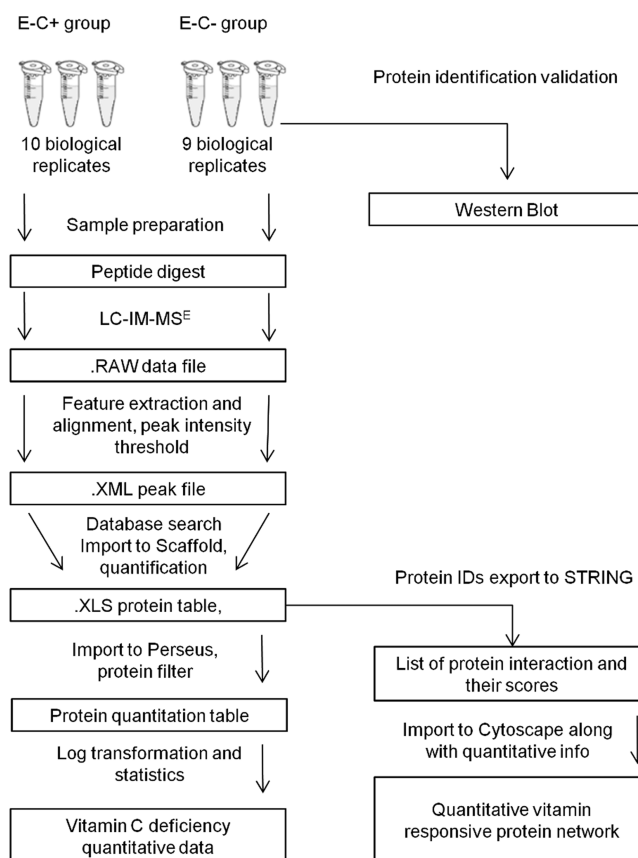

Figure 1. Data analysis workflow for label-free quantitative proteomics using LC−IMS−MS^E acquisitions. We implemented MassLynx and PLGS for peak extraction, alignment, and database search; Scaffold for spectra validation and protein quantitation; Perseus for statistical analysis; and STRING and Cytoscape for protein interactions analysis and network construction.

commercially available software package can perform only a few steps of the data analysis pipeline (Figure 1). Here we implemented MassLynx and PLGS for peak extraction, alignment, and database search; Scaffold for spectra validation and protein quantitation; Perseus for statistical analysis; and STRING and Cytoscape for protein interactions analysis and network construction, respectively.

Effects on Body Weight and Growth Rate

The experimental design of the feeding study afforded that zebrafish of the E+C− and E−C− groups were harvested after 98 days and the E−C+ and E+C+ groups were sacrificed after 119 days. We therefore expected that the different groups would result in different median fish body weights. Indeed, as shown in the Supporting Information, Figure S3A, the median fish weights were lower for E+C− and E−C−groups compared with E−C+ and E+C+ groups. The ANOVA test between all four groups did not show significant results, but the median body weights were significantly different between the E+C+ and E−C− groups (p value = 0.006, t test). Also, not totally unexpected, the growth rate (median body mass/age) of fish adequate in both vitamins (E+C+ group) was approximately three times higher compared with the group deficient in both vitamins (E−C− group). Vitamin C deficiency seemed to have a more drastic effect on the growth rate compared with inadequate vitamin E levels (Supporting Information, Figure S3B).
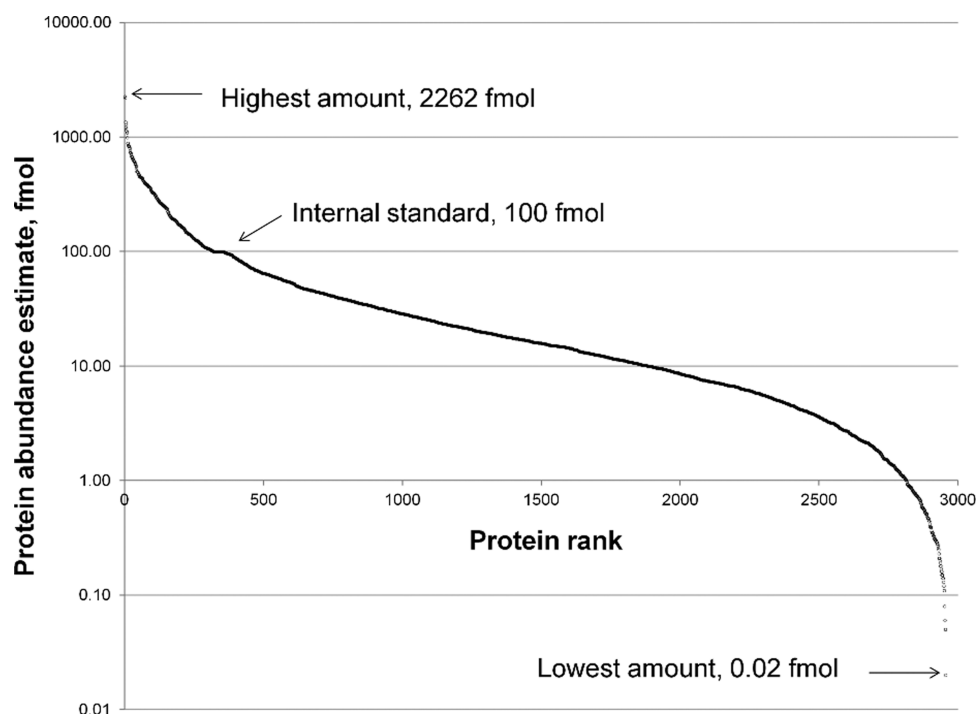
Figure 2. Dynamic range of the method based on protein abundance estimates. The plot has the predicted S-shape, and the quantitative dynamic range covers five orders of magnitude based on 2956 data points derived from LC−IM−MS^E data of all 37 samples. The value for the detection limit was identified as the lowest amount of a protein calculated by Scaffold software. The detection limit of this method was as low as 20 amol (Heat shock protein 8, sample E+C+#5), while the highest detected amount was 2.3 pmol (Myosin light chain, sample E−C+#8).

Optimization of Sample Preparation and Analytical Workflow for the Comparative "Bottom-up" Proteomics Study

To account for differences in fish body weights, we normalized the total protein concentration, which resulted in solutions with equal total concentration of proteins independent of fish weights, age, and vitamin supplementation. The total protein concentration in each sample was verified to confirm the validity of the sample preparation technique and for further use. The median total concentration of proteins for all samples was 2.382 mg/mL with first quartile 2.258 mg/mL and third quartile 2.478 mg/mL. As was expected from the sample preparation that accounted for the differences in fish weights, the total concentration of proteins was distributed in a narrow range (Supporting Information, Figure S4). After lysis, insoluble pellets that remained in the microcentrifuge tubes were discarded. The supernatant was used for protein digestion.

Because of the complexity of the whole fish protein extracts, we optimized the LC conditions to increase the number of peptides detected.[49] For optimization, a protein extract was run using different LC gradients, and the number of eluted peptides was compared. By changing the mobile phase composition over time, the gradient was optimized after each run to make the elution of peptides even across a chromatogram and to reduce the coelution of peptides. The gradients were named as "Gradient 1", "Gradient 2", "Gradient 3", and "Gradient 4". The gradient profiles and respective chromatograms are presented in the Supporting Information, Figure S5. Using Venn diagrams, a comparison of the number of eluted peptides for each gradient is presented in the Supporting Information, Figure S6. "Gradient 4" resulted in the highest number of peptides detected and was used for all following LC−IM−MS^E analyses.

Data Analysis Strategy Used for Obtaining Protein Abundance Estimates

Label-free approaches are liable to technical variability, such as LC retention time drift, nanospray instability, and sample matrix effects. Therefore, to overcome these caveats, label-free approaches depend on the use of an internal standard and the application of proper mathematical tools for data processing. Log transformation of data is commonly used to make the distribution of protein abundances more Gaussian, with subsequent application of parametric statistical tests, which have higher statistical power after data transformation.[50]

In this study, a digest of enolase from *Saccharomyces cerevisiae* was used as an internal standard. The same volume of the internal standard was added to each sample, making its concentration equal across samples. Data were acquired, deisotoped, peak-aligned, and exported to Scaffold for quantitative analysis. The quantification of proteins was done by normalization of the protein abundances to the internal standard. For the total of 2956 quantitative values obtained, a graph of protein amounts of the identified proteins from all samples against protein ranks was created (Figure 2). The value for the detection limit was extracted as the lowest amount of a protein that was calculated by Scaffold. The detection limit of this method was as low as 20 amol (Heat shock protein 8, sample E+C+#5), while the highest detected concentration was 2.3 pmol (Myosin light chain, sample E−C+#8). The dynamic range of estimates of protein amounts was calculated to be about five orders of magnitude.

Next, data were exported to Perseus and log$_2$-transformed. To estimate the biological variation between fish samples, we calculated the coefficient of determination, R^2, based on the protein estimates between biological replicates. As an example, Supporting Information Figure S7 shows the correlation plot
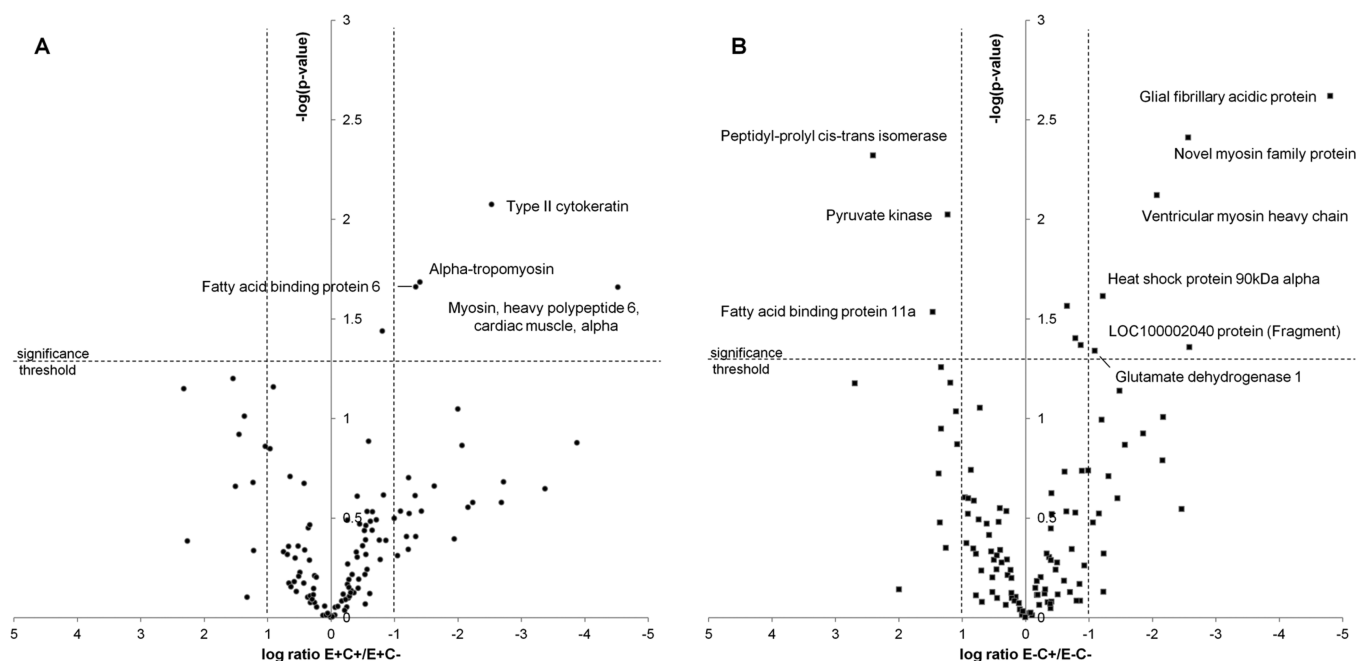
Figure 3. Volcano plot representation of protein abundance changes caused by vitamin C deficiency. Side-by-side comparison of the volcano plots of protein abundance changes reveals the permissive role of vitamin E in vitamin-C-deficient fish. In the group low in vitamin E, the lack of vitamin C causes changes in proteins associated with pathways of energy metabolism (pyruvate kinase and glutamate dehydrogenase) and other protein with roles in stress response.

between the biological replicates E−C+ #9 and E−C+ #8 resulting in a R^2 value of 0.654. Additional correlation plots for the E−C+ group are shown in Supporting Information Figure S8. As expected, variation between samples was observed. The correlation of protein amounts between different fish (within one feeding group) was found to be stronger in samples containing higher numbers of proteins.

Proteome Changes Linked to Vitamin C Deficiency

To investigate the proteome changes caused by vitamin C deficiency in vitamin-E-adequate fish, we evaluated the fold changes of the protein estimates obtained for the E+C+ versus the E+C− group. For quantitative analysis, peptide identifications were accepted if they could be established at a >95% probability. Protein identifications were accepted if they could be established at >99.0% probability and contained at least two identified peptides. The quantitative values calculated for the comparison of groups C+ versus C− (both sufficient in vitamin E) were based on 8134 spectra with peptide FDR 0.1% and 203 protein with protein FDR 2.0%. Next, internal standard and contaminants were removed and quantitation filter was applied. All proteins that were not detected at least two times across a group were filtered out. This conservative approach resulted in 119 proteins. Among them, 61% were up-regulated in vitamin-C-deficient fish (72 of 119). A change in concentration of two-fold or more was observed for 28% of the proteins in this group.

The same quantitative analysis was done to investigate the proteome changes caused by vitamin C deficiency in vitamin-E-deficient fish. For quantitative analysis, peptide identifications were accepted if they could be established at a >50% probability. Protein identifications were accepted if they could be established at >99.9% probability and contained at least two identified peptides. The quantitative values calculated for the comparison of the C+ versus C− group (both deficient in vitamin E) were based on 11 308 spectra with peptide FDR

0.2% and 221 protein with protein FDR 2.3%. Again, internal standard and contaminants were removed and quantitation filter was applied. This resulted in a list of 112 proteins (Supplementary Table S3 in the Supporting Information). Among them, 52% were up-regulated in vitamin-C-deficient fish (58 of 112). A change in concentration of two-fold or more was observed for 29% of the proteins.

Figure 3A shows a volcano plot for the distribution of p values versus fold-changes calculated for the proteins that were assigned for the comparison of the E+C+ versus E+C− groups (E+C+/E+C− transition). A negative logarithm of the p values and the logarithm of the ratio between amount of proteins from E+C+ and E+C− groups are displayed on the y and x axes, respectively. Dashed lines show a cutoff of two-fold change and a p-value threshold of 0.05 to define differential regulation of proteins between groups. Four proteins, namely, type-II cytokeratin, alpha tropomyosin, myosin heavy polypeptide 6, and fatty acid binding protein 6, showed a significant change upon vitamin C deficiency in vitamin-E-adequate fish, and all were upregulated. Regulation of alpha tropomyosin by α-tocopherol aligns well with previously published data.[51]

In the Figure 3B, the volcano plot is shown for evaluating differential regulation of proteins in group E−C+ versus group E−C− (E−C+/E−C− transition). We found that three proteins were down-regulated (pyruvate kinase M2b, fatty acid binding protein 11, and peptidyl-prolyl cis−trans isomerase) and six up-regulated (glial fibrillary acidic protein, ventricular myosin heavy chain, glutamate dehydrogenase 1, heat shock protein 90 kDa alpha, LOC100002040 protein, and novel myosin family protein CH211-158M24.10-001) as a consequence of vitamin C deficiency in vitamin-E-deficient fish.

A side-by-side comparison of the two volcano plots reveals the permissive role of vitamin E in the effect of vitamin C deficiency on the fish. In the vitamin-E-deficient fish the additional lack of vitamin C causes changes in expression levels
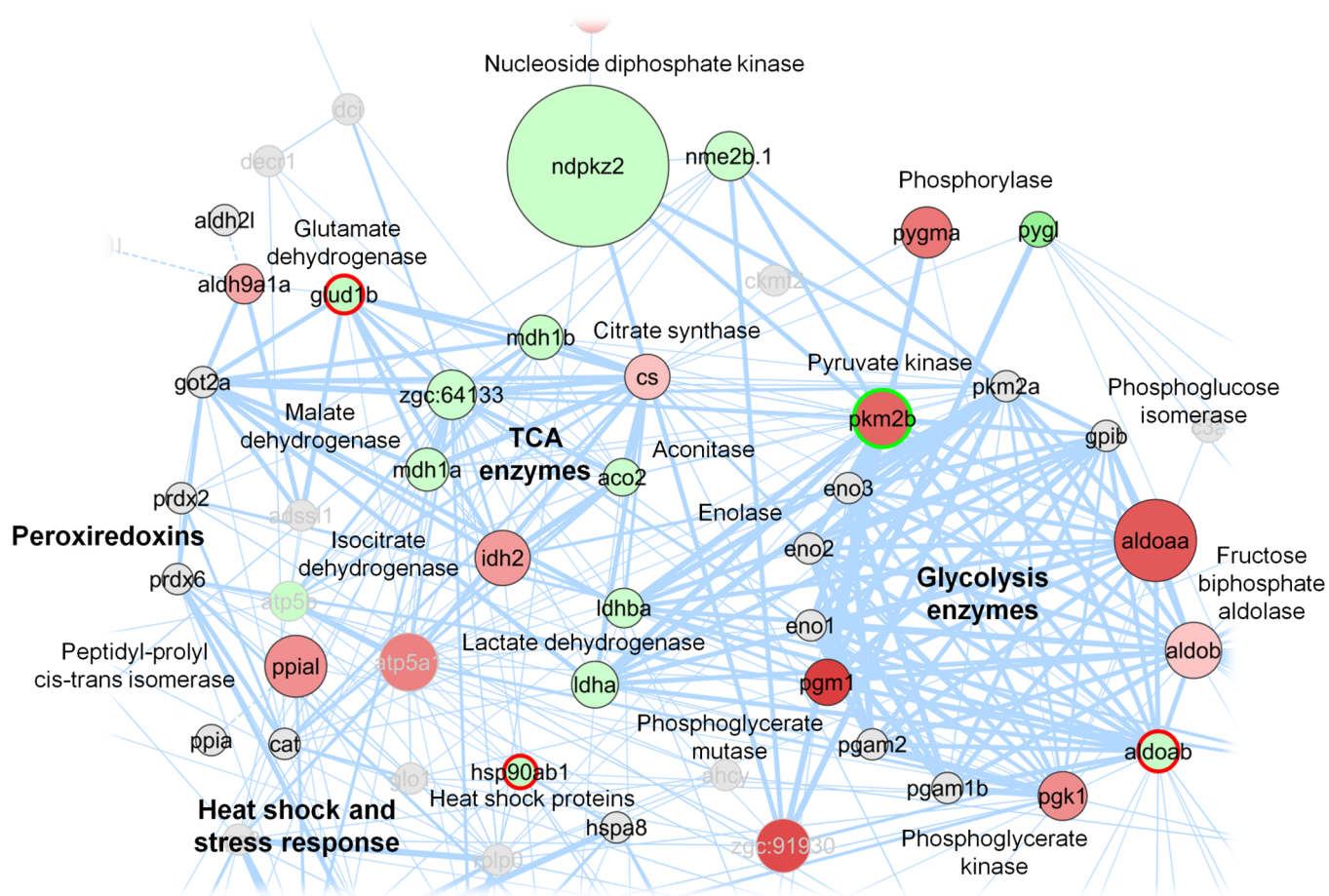
Figure 4. Protein−protein interaction network visualization of subnetworks that contain proteins that showed changes in expression levels upon vitamin C deficiency in the vitamin-E-deficient state. In the network each node represents a protein found in either group E−C+ or E−C−. The change in protein amounts between vitamin-C-adequate and -deficient fish is color-coded: green nodes represent proteins that increased their amounts, red represents those that decreased; gray nodes show proteins that were not quantified. The size of a node represents an average of the protein abundance estimates in the E+C− group. The width of a line connecting proteins represents the strength of proteins interaction, as extracted from STRING software. Subnetworks of proteins involved in glycolysis and the TCA cycle are highlighted as well as proteins associated with stress response.

of proteins responsible for energy metabolism, namely, pyruvate kinase and glutamate dehydrogenase, along with other marker proteins. To obtain functional insight into proteins and pathways that are affected by vitamin C deficiency, we functionally annotated the combined proteomic data sets of the E−C− and E−C+ groups using the Gene Ontology (GO) classification (Supporting Information, Table S4).

Responsive Protein Interaction Network of Vitamin C Deficiency

A protein interaction network was constructed to provide a comprehensive visualization of the proteins identified, their abundance estimates, as well as differential regulation caused by vitamin C deficiency in fish low on vitamin E (Supporting Information, Figure S9). In the network, each node represents a protein found in either group E−C+ or E−C−. The change in protein amounts between vitamin-C-adequate and -deficient fish is color coded: green nodes represent proteins that increased their amounts, red represent those that decreased, and gray nodes show proteins that were not quantified. The size of a node represents an average of the protein abundance estimates in the E−C− group. The width of a line connecting proteins represents the strength of proteins interaction, as extracted from STRING. Figure 4 provides a closer look at

subnetworks that encompassed proteins that were differentially regulated in response to vitamin E and C deficiency. Upregulated proteins were members of the subnetworks representing glutaminolysis, TCA cycle, and stress response.

Biological Inferences of Altered Protein Expressions in Vitamin-E- and -C-Deficient Zebrafish

The interaction network highlights the modulation of several proteins involved in two interconnected metabolic pathways, the glycolysis and TCA cycle (Figure 5). Proteins are shown as upregulated (green arrow up), downregulated (red arrow down), unquantified (gray arrow), and not detected (no arrow) with their respective numerical fold changes (Supporting Information, Table S4). Proteins that showed a statistically significant fold change are marked with an asterisk.

Upon vitamin C deficiency in groups low on vitamin E, glycolytic enzymes were downregulated. The last step in the glycolysis pathway involves a transfer of the phosphate group from phosphoenolpyruvate to ADP, producing a molecule of pyruvate and a molecule of ATP. This step is catalyzed by pyruvate kinase (PK), which was significantly downregulated in vitamin-E- and -C-deficient fish (p value = 0.009, t test for log-transformed data). In humans and other mammals, four isoforms of pyruvate kinase are expressed: the L and R
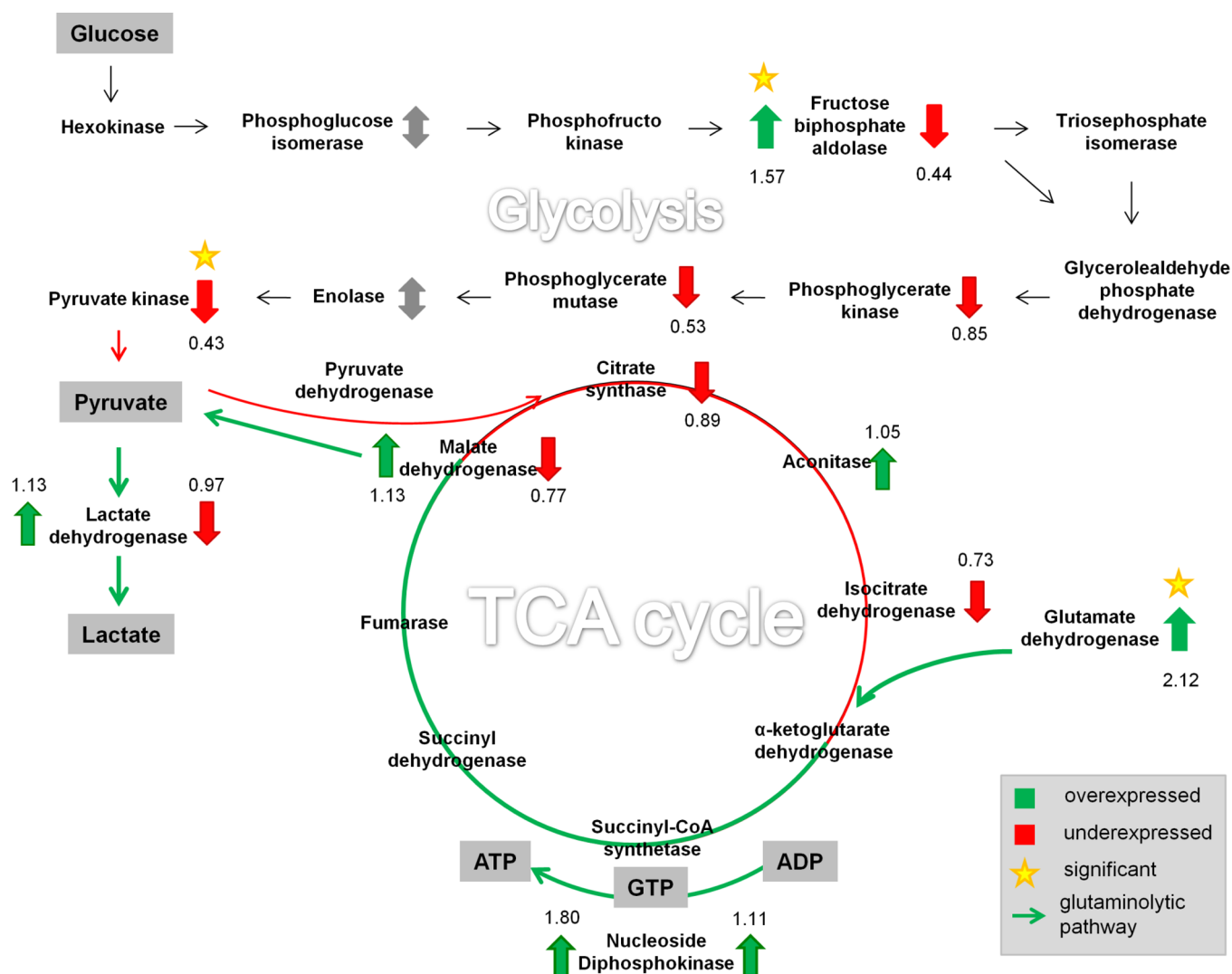
Figure 5. Schematic of the metabolic pathways that were associated with proteins that showed changes in abundance estimates as a consequence of vitamin C deficiency. To analyze the consequences of vitamin C deficiency, we combined quantitative data with metabolic pathways linked to energy production, namely, glycolysis, TCA cycle, and glutaminolysis. Proteins that were upregulated are indicated by a green arrow up, downregulated proteins are marked with a red arrow down, detected but not quantified proteins are marked with a double arrow in gray, and not detected proteins are unmarked. Proteins are labeled with their respective numerical fold-changes observed for vitamin C deficiency (in the vitamin-E-deficient group). Proteins that showed a statistically significant fold change are marked with an asterisk.

isoforms are found in liver and red blood cells, the M1 isoform is expressed in most adult tissues, and the M2 isoform, a splice variant of M1, is the predominant form found in proliferating cells and tumor cells.[52,53] In the current study, pyruvate kinase M2 was detected but not M1 nor L/R. Western Blot analysis confirmed the presence and change of pyruvate kinase M2 (data not shown). Under the conditions of suppressed glycolysis there will be less production of energy (ATP) and reducing power (NADH), the main products of the cycle. We may therefore speculate that in vitamin-E- and -C-deficient fish compensatory mechanisms for the production of energy are activated. Kirkwood et al. studied vitamin-C-deficient zebrafish at the metabolome level and reported activation of the purine nucleotide cycle as possible compensatory mechanism to satisfy intracellular ATP requirements.[29]

After conversion of glutamine to glutamate, glutamate dehydrogenase catalyzes the production of α-ketoglutarate, which subsequently enters the TCA cycle. The conversion of glutamine to lactate is commonly referred as glutaminoly-

sis.[54,55] Our quantitative proteomic study indicates that several proteins that play key roles in glutaminolysis are elevated in vitamin-E- and -C-deficient fish (E−C− group). Our data sets show a significant increase in levels of glutamate dehydrogenase (Glud1b) under vitamin E and C deficiency compared with E deficiency alone (p value = 0.046, t test for log-transformed data). The change in this protein was confirmed with Western Blot (data not shown). Malate dehydrogenase and lactate dehydrogenase, enzymes involved in glutaminolysis, were increased as well. The elevation of several key enzymes involved in glutaminolysis supports the notion that vitamin E and C deficiency promotes a metabolic phenotype in which glutaminolytic pathways are activated for alternative energy production (ATP) and reducing power (NADPH) in cells under conditions of suppressed glycolysis.

In addition, our quantitative proteomics screens revealed that Glial fibrillary acidic protein (Gfap) was significantly elevated (27 times) in fish deficient in both vitamins (p value = 0.002, t test for log transformed data), while there was no significant

difference in Gfap expression between E+C+ and E−C+ groups consistent with the notion that vitamin E seems to exhibit a permissive role in governing the proteome biology of adult zebrafish. The adverse effect of deficiency of both vitamins has been previously reported.[2] The identification of Gfap was based on a conservative probability for protein identification of at least 85% and at least two unique peptides with peptide identification probability of at least 50%. The similarity between zebrafish and human Gfap (GFAP_HUMAN, entry P14136 in Uniprot) is 65%, as calculated by Blast search. Despite the good homology of the human and zebrafish protein, the human antibody used in the Western blot analyses showed nonspecific binding and Western blots were not conclusive. Gfap is a recognized marker of neurologic injury and trauma and is released during astrogliosis in higher vertebrates.[56−58]

CONCLUSIONS

We applied a label-free comparative proteomics approach for examining the systems-wide consequences of insufficient levels of two essential micronutrients, vitamins E and C, in adult zebrafish. The experimental design adopted allowed the study of vitamin C deficiency at the whole organism level. Using a label-free quantitative proteomic workflow, it was possible to assess for the first time changes in the vertebrate proteome upon vitamin C deficiency. The label-free quantitative bottom-up strategy with LC−ion mobility−MS^E is a powerful approach to determine protein abundance estimates in zebrafish. We report sensitivity of the method as low as 20 amol and a dynamic range of five orders of magnitude for protein level estimates. Our results indicate the modulation of expression of proteins involved in stress response and metabolic pathways associated with energy production. Our findings suggest that severe vitamin C deficiency potentiated by vitamin E deficiency causes the suppression of glycolysis and the activation of glutaminolysis as an alternative way to fulfill cellular energy requirements. Glial fibrillary acidic protein (Gfap) showed a significant overexpression in fish low in both vitamins C and E, proving that severe vitamin C deficiency in combination with low vitamin E status causes injury of the central nervous system.

ASSOCIATED CONTENT

Supporting Information

Table S1: Pipetting scheme used for sample lysis and preparation of digests. Table S2: Synapt G2 HDMS instrument settings used for Ion-Mobility-MS^E acquisitions. Table S3: The number of peptides and proteins assigned in each of the biological samples subjected to LC−IM−MS^E analysis. Table S4: Proteins identified in the E−C+ and the E−C− groups, GO annotations and fold-changes observed in the vitamin-C-deficient fish (E−C−/E−C+ transition). Table S5: Protein Table for Study (A) E+C+ versus E+C− and (B) E−C+ versus E−C−: Compilation of proteins found in each samples, unique peptides identified per protein, and respective sequence coverage. Figure S1: Design of the feeding experiment. Figure S2: Workflow used for preparing the samples for the label-free "bottom-up" quantitative proteomics study. Figure S3: Fish characteristics dependent on the vitamin regime fed. Figure S4: A boxplot of the distribution of the total protein concentration after extraction and lysis. Figure S5: Gradient profiles with respective base peak chromatograms. Figure S6: Venn diagrams comparing the number of peptides eluting from a column and

identified with LC−IM−MS^E. Figure S7: Correlation plot between E−C+ sample 9 and E−C+ sample 8. Figure S8: Correlation plot matrix of the E−C+ group. Figure S9: The responsive protein network for the vitamin transition C+/C− and both groups deficient in vitamin E status (E−C+ vs E−C+). This material is available free of charge via the Internet at http://pubs.acs.org.

AUTHOR INFORMATION

Corresponding Author

*E-mail: claudia.maier@oregonstate.edu.

Notes

The authors declare no competing financial interest.

ACKNOWLEDGMENTS

REFERENCES

(1) Burk, R. F.; Christensen, J. M.; Maguire, M. J.; Austin, L. M.; Whetsell, W. O.; May, J. M.; Hill, K. E.; Ebner, F. F. *J. Nutr.* **2006**, *136*, 1576−1581.

(2) Hill, K. E.; Montine, T. J.; Motley, A. K.; Li, X.; May, J. M.; Burk, R. F. *Am. J. Clin. Nutr.* **2003**, *77*, 1484−8.

(3) Lebold, K. M.; Löhr, C. V; Barton, C. L.; Miller, G. W.; Labut, E. M.; Tanguay, R. L.; Traber, M. G. *Comp. Biochem. Physiol., Part C: Toxicol. Pharmacol.* **2013**, *157*, 382−9.

(4) Buettner, G. R.; Schafer, F. Q. *Teratology* **2000**, *62*, 234.

(5) Halliwell, B. *Free Radic. Res.* **1999**, 261−72.

(6) Kalyanaraman, B.; Darley-Usmar, V. M.; Wood, J.; Joseph, J.; Parthasarathy, S. *J. Biol. Chem.* **1992**, *267*, 6789−95.

(7) Bruno, R. S.; Leonard, S. W.; Atkinson, J.; Montine, T. J.; Ramakrishnan, R.; Bray, T. M.; Traber, M. G. *Free Radic. Biol. Med.* **2006**, *40*, 689−97.

(8) Buettner, G. *Arch. Biochem. Biophys.* **1993**, 535−43.

(9) Peterkovsky, B.; Undenfriend, S. *Proc. Natl. Acad. Sci. U. S. A.* **1965**, *53*, 335−42.

(10) Myllylä, R.; Kuutti-Savolainen, E.-R.; Kivirikko, K. I. *Biochem. Biophys. Res. Commun.* **1978**, *83*, 441−448.

(11) Diaz, M. N.; Frei, B.; Vita, J. A.; Keaney, J. F. *N. Engl. J. Med.* **1997**, *337*, 408−16.

(12) Wilson, J. X. *Biofactors* **2009**, *35*, 5−13.

(13) Armour, J.; Tyml, K.; Lidington, D.; Wilson, J. X. *J. Appl. Physiol.* **2001**, *90*, 795−803.

(14) Piyathilake, C. J.; Macaluso, M.; Hine, R. J.; Vinter, D. W.; Richards, E. W.; Krumdieck, C. L. *Cancer Epidemiol. Biomarkers Prev.* **1995**, *4*, 751−8.

(15) Frikke-Schmidt, H.; Tveden-Nyborg, P.; Birck, M. M.; Lykkesfeldt, J. *Br. J. Nutr.* **2011**, *105*, 54−61.

(16) Bánhegyi, G.; Braun, L.; Csala, M.; Puskás, F.; Mandl, J. *Free Radic. Biol. Med.* **1997**, *23*, 793−803.

(17) Chatterjee, I. B.; Majumder, A. K.; Nandi, B. K.; S., N. *Ann. N.Y. Acad. Sci.* **1975**, 24−47.

(18) Delanghe, J. R.; Langlois, M. R.; De Buyzere, M. L.; Na, N.; Ouyang, J.; Speeckaert, M. M.; Torck, M. a *Genes Nutr.* **2011**, *6*, 341−6.

(19) Nishikimi, M.; Fukuyama, R.; Minoshima, S.; Shimizu, N.; Yagi, K. *J. Biol. Chem.* **1994**, *269*, 13685−8.

(20) Grollman, A. P.; Lehninger, A. L. *Arch. Biochem. Biophys.* **1957**, *69*, 458−467.

(21) Harrison, F. E.; Meredith, M. E.; Dawes, S. M.; Saskowski, J. L.; May, J. M. *Brain Res.* **2010**, *1349*, 143−52.

(22) Telang, S.; Clem, A. L.; Eaton, J. W.; Chesney, J. *Neoplasia* **2007**, *9*, 47−56.

(23) Dabrowski, K. *Biol. Chem. Hoppe-Seyler* **1990**, *371*, 207–14.

(24) Touhata, K.; Toyohara, H.; Mitani, T.; Kinoshita, M.; Satou, M.; Sakaguchi, M. *Fish. Sci.* **1995**, *61*, 729–730.

(25) Toyohara, H.; Nakata, T.; Touhata, K.; Hashimoto, H.; Kinoshita, M.; Sakaguchi, M.; Nishikimi, M.; Yagi, K.; Wakamatsu, Y.; Ozato, K. *Biochem. Biophys. Res. Commun.* **1996**, *223*, 650–3.

(26) Phromkunthong, W.; Storch, V.; Braunbeckw, T. *J. Appl. Ichthyol.* **1994**, *10*, 146–153.

(27) Dabrowski, K.; Ciereszko, A. *Experientia* **1996**, *52*, 97–100.

(28) Drouin, G.; Godin, J.-R.; Pagé, B. *Curr. Genomics* **2011**, *12*, 371–8.

(29) Kirkwood, J. S.; Lebold, K. M.; Miranda, C. L.; Wright, C. L.; Miller, G. W.; Tanguay, R. L.; Barton, C. L.; Traber, M. G.; Stevens, J. F. *J. Biol. Chem.* **2012**, *287*, 3833–41.

(30) Brigelius-Flohe, R.; Traber, M. G. *FASEB J.* **1999**, *13*, 1145–1155.

(31) Traber, M. G.; Atkinson, J. *Free Radic. Biol. Med.* **2007**, *43*, 4–15.

(32) McCormack, A. L.; Schieltz, D. M.; Goode, B.; Yang, S.; Barnes, G.; Drubin, D.; Y., J., 3rd. *Anal. Chem.* **1997**, *69*, 767–76.

(33) Peng, J.; Elias, J. E.; Thoreen, C. C.; Licklider, L. J.; G., S. *J. Proteome Res.* **2003**, *2*, 43–50.

(34) Washburn, M. P.; Wolters, D.; Yates, J. R. *Nat. Biotechnol.* **2001**, *19*, 242–7.

(35) Voyksner, R. D.; Lee, H. *Rapid Commun. Mass Spectrom.* **1999**, *13*, 1427–37.

(36) Purves, R. W.; Gabryelski, W.; Li, L. *Rapid Commun. Mass Spectrom.* **1998**, *12*, 695–700.

(37) Croker, C. G.; Pearcy, J. O.; Stahl, D. C.; Moore, R. E.; Keen, D. A.; Lee, T. D. *J. Biomol. Tech.* **2000**, *11*, 135–141.

(38) Plumb, R. S.; Johnson, K. A.; Rainville, P.; Smith, B. W.; Wilson, I. D.; Castro-perez, J. M.; Nicholson, J. K. *Rapid Commun. Mass Spectrom.* **2006**, 1989–1994.

(39) Geromanos, S. J.; Vissers, J. P. C.; Silva, J. C.; Dorschel, C. a; Li, G.-Z.; Gorenstein, M. V; Bateman, R. H.; Langridge, J. I. *Proteomics* **2009**, *9*, 1683–95.

(40) Silva, J. C.; Denny, R.; Dorschel, C.; Gorenstein, M. V; Li, G.-Z.; Richardson, K.; Wall, D.; Geromanos, S. J. *Mol. Cell. Proteomics* **2006**, *5*, 589–607.

(41) Ritter, S. *Chem. Eng. News* **2007**, *85*, 61–65.

(42) Salbo, R.; Bush, M. F.; Naver, H.; Campuzano, I.; Robinson, C. V; Pettersson, I.; Jørgensen, T. J. D.; Haselmann, K. F. *Rapid Commun. Mass Spectrom.* **2012**, *26*, 1181–93.

(43) Hoaglund-Hyzer, C. S.; Li, J.; Clemmer, D. E. *Anal. Chem.* **2000**, *72*, 2737–40.

(44) Miller, G. W.; Labut, E. M.; Lebold, K. M.; Floeter, A.; Tanguay, R. L.; Traber, M. G. *J. Nutr. Biochem.* **2012**, *23*, 478–486.

(45) Keller, A.; Nesvizhskii, A. I.; Kolker, E.; Aebersold, R. *Anal. Chem.* **2002**, *74*, 5383–5392.

(46) Nesvizhskii, A. I.; Keller, A.; Kolker, E.; Aebersold, R. *Anal. Chem.* **2003**, *75*, 4646–4658.

(47) Szklarczyk, D.; Franceschini, A.; Kuhn, M.; Simonovic, M.; Roth, A.; Minguez, P.; Doerks, T.; Stark, M.; Muller, J.; Bork, P.; Jensen, L. J.; Von Mering, C. *Nucleic Acids Res.* **2011**, *39*, D561–8.

(48) Smoot, M. E.; Ono, K.; Ruscheinski, J.; Wang, P.-L.; Ideker, T. *Bioinformatics* **2011**, *27*, 431–432.

(49) Righetti, P. G.; Castagna, A.; Herbert, B.; Reymond, F.; Rossier, J. S. *Proteomics* **2003**, *3*, 1397–407.

(50) Ramsey, F. L.; Schafer, D. W. *The Statistical Sleuth: A Course in Methods of Data Analysis*; Cengage Learning: Boston, 2012; p 760.

(51) Azzi, A.; Breyer, I.; Feher, M.; Ricciarelli, R.; Stocker, A.; Zimmer, S.; Zingg, J. *J. Nutr.* **2001**, *131*, 378S–81S.

(52) Jurica, M. S.; Mesecar, A.; Heath, P. J.; Shi, W.; Nowak, T.; Stoddard, B. L. *Structure* **1998**, *6*, 195–210.

(53) Mazurek, S.; Boschek, C. B.; Hugo, F.; Eigenbrodt, E. *Semin. Cancer Biol.* **2005**, *15*, 300–8.

(54) DeBerardinis, R. J.; Mancuso, A.; Daikhin, E.; Nissim, I.; Yudkoff, M.; Wehrli, S.; Thompson, C. B. *Proc. Natl. Acad. Sci. U. S. A.* **2007**, *104*, 19345–50.

(55) Le, A.; Lane, A. N.; Hamaker, M.; Bose, S.; Gouw, A.; Barbi, J.; Tsukamoto, T.; Rojas, C. J.; Slusher, B. S.; Zhang, H.; Zimmerman, L. J.; Liebler, D. C.; Slebos, R. J. C.; Lorkiewicz, P. K.; Higashi, R. M.; Fan, T. W. M.; Dang, C. V *Cell Metab.* **2012**, *15*, 110–21.

(56) Vos, P. E.; Lamers, K. J. B.; Hendriks, J. C. M.; van Haaren, M.; Beems, T.; Zimmerman, C.; van Geel, W.; de Reus, H.; Biert, J.; Verbeek, M. M. *Neurology* **2004**, *62*, 1303–10.

(57) Eng, L. F.; Ghirnikar, R. S.; Lee, Y. L. *Neurochem. Res.* **2000**, *25*, 1439–51.

(58) Schiff, L.; Hadker, N.; Weiser, S.; Rausch, C. *Mol. Diagn. Ther.* **2012**, *16*, 79–92.